Quantum Computation of Fluid Dynamics

Jeffrey Yepez

yepez@plh.af.mil

http://hadron.plh.af.mil

Air Force Research Laboratory, Hanscom Field, Massachusetts, 01731

Februrary 16, 1998

Abstract

Presented is a quantum lattice gas for Navier-Stokes fluid dynamics simulation. The quantum lattice-gas transport equation at the microscopic scale is presented as a generalization of the classical lattice-gas transport equation. A special type of quantum computer network is proposed that is suitable for implementing the quantum lattice gas. The quantum computer network undergoes a partial collapse of the wavefunction at every time step of the dynamical evolution. Each quantum computer in the network comprises only a few qubits, which are entangled for only a short time period. A Chapman-Enskog type analysis of the quantum computer network indicates that the total system of qubits behaves exactly like a viscous lattice-gas fluid at the macroscopic scale. Because of the quantum mechanical nature of the scattering process, superposition of outgoing collisional possibilities occurs. The quantum lattice gas obeys detail balance in its collisions and is therefore an unconditionally stable algorithm for fluid dynamics simulation.

1   Introduction

Prior to the advent of digital computing in the late 1940's, analog computers held much promise. An electrical circuit can be constructed to simulate, say, an underdamped oscillator governed by a second order differential equation. For example, an electrical circuit can drive a trace on an oscilloscope mimicking the vertical motion response of a fast moving automobile with poor shock absorbers after passing over a speed bump—one continuous physical system configured to behave just like another continuous physical system. Today, after five decades of digital computing, history may repeat itself in the sense that it may again be

worthwhile to build "analog" computers—for example, a quantum mechanical spin system configured to behave just like a Navier-Stokes fluid.

The purpose of this paper is to show how to do this. We show how to arrange a network of small quantum computers so that, taken as a system, the qubits within the network mimic the behavior of a system of massive quantum particles moving and colliding on a discrete spacetime lattice. This discrete quantum particle system is termed a *quantum lattice gas* and the associated quantum computer network is called a *lattice-gas quantum computer*.

Over a decade ago, classical lattice gases were found that behave like a viscous Navier-Stokes fluid at the macroscopic scale [1, 2]. In this paper we show that a quantum lattice gas does too. The prediction of the quantum lattice gas' macroscopic equations of motion is achieved by a generalized Chapman-Enskog analysis. A property of the quantum lattice gas (when used as a numerical algorithm to implement a probabilistic lattice gas on a classical computer) is that continuous macroscopic fields for the mass and momentum densities are directly obtained. There is no need for either ensemble averaging or coarse-grain space-time averaging, which are computationally expensive in a classical lattice-gas simulation. This computationally useful property of the quantum lattice gas arises because it models the discrete particle system directly at the mesoscopic scale, avoiding noisy fluctuations while retaining detailed balance in the local particle collisions [3]. Detailed balance is satisfied because of the unitary action of the collision operator as it causes quantum mechanical superpositions of outgoing particle configurations at each site of the spatial lattice. Consequently, the quantum lattice gas is unconditionally stable as a numerical algorithm.

We calculate the single-particle distribution function analytically for a quantum lattice-gas system at local equilibrium. The analytical prediction is that it has the same form as the single-particle distribution function of a classical lattice-gas system, which also obeys the principle of detailed balance. We verify this prediction through numerical simulation of a two-dimensional quantum lattice gas, which is a straightforward generalization of the classical FHP lattice gas [2]. For comparison purposes, we also include results from a classical FHP simulation. In the low Mach number incompressible fluid regime, there is excellent agreement between the theoretical prediction and the numerical data for the single-particle occupation probability.

2   Review

There are new possibilities and limitations that arise in computing if we use the principle of quantum mechanical superposition of states [4, 5, 6, 7, 8, 9]. In quantum computing a two-level quantum bit represents the smallest unit of information which may be in a superposition of the discrete states $|0\rangle$ and $|1\rangle$.[1] An example of the physical embodiment of a qubit is the z-component of

---

[1]A qubit, $|q\rangle = \alpha|0\rangle + \beta|1\rangle$, has an amplitude, α, of it being in the *zero state*, $|0\rangle$, and another amplitude, β, of finding it in the *one state*, $|1\rangle$. The probabilities add to unity: $\langle 0|0\rangle + \langle 1|1\rangle = \langle q|q\rangle$ so the complex coefficients are constrained by $|\alpha|^2 + |\beta|^2 = 1$.

a nuclear spin in an atom in a uniform external magnetic field.[2]

An open issue for quantum computing is whether entangled qubit states (of many qubits, much more than two) can be isolated from the surrounding environment for delicate quantum algorithmic steps to be completed. Using quantum mechanical superposition among qubit states to speedup a computation by simultaneously encoding many possibilities, an approach termed *quantum parallelism*, is generally considered the primary virtue of quantum computation.[3] Yet uncontrolled coupling with the surrounding environment causes decoherence of the qubit states and the virtue is lost—quantum parallelism levies a high price for coherence of the quantum computer's wavefunction. This has spurred the development of scalable quantum error correction techniques, considered crucially important for the enterprise to continue [11, 8, 12, 13]. Because of the difficulties of quantum coherence, the first quantum computer comprised only two qubits.

An historical starting point that led to quantum computing was reversible computing [14]. Since microscopic physics is reversible[4], it is believed that quantum mechanical algorithms must be too.[5] Reversible algorithms for simulating physics on a quantum device can serve as a guide for constructing the device. The common assumption is the quantum mechanical device itself undergoes unitary (and therefore reversible) evolution as it transitions through its "computation".[6]

For any reversible computation, one can describe the algorithm by specifying a unitary evolution operator, formally written as $e^{i\hat{H}\tau/\hbar}$, acting on the system wavefunction, $|\Psi\rangle$, which constitutes the state of the quantum computer's "memory". With N qubits, the quantum state $|\Psi\rangle$ resides in an exponentially large Hilbert space with 2^N dimensions. A new quantum state, $|\Psi'\rangle$, is generated by application of a unitary matrix of size $2^N \times 2^N$ as follows

$$|\Psi'\rangle = e^{i\hat{H}\tau/\hbar}|\Psi\rangle. \tag{1}$$

By repeated application of $e^{i\hat{H}\tau/\hbar}$ an ordered sequence of states is generated and each one is given a unique time label. If the first state is labeled by t then the next one is labeled by $t + \tau$, and the next by $t + 2\tau$, and so forth. With this

---

[2]Cory *et al.* have employed the quantum number m_x of a nuclear spin of an atom in a molecule of a liquid placed in a strong external magnetic field to encode a single qubit and they used nuclear magnetic resonance to control its state and interaction with qubits in neighboring atoms within the same molecule [10].

[3]In lattice-gas quantum computation, quantum parallism is used to allow for simultaneous multiple collision possibilities at each site of the lattice. This allows for a reduction in the viscosity of the fluid that improves the computational efficiency. Yet the computational efficiency is also due to the continuous phase of the qubit, $|q\rangle = \cos\theta|1\rangle + \sin\theta|0\rangle$, which we use to represent the probability of finding a particle, $f_a = \cos^2\theta$.

[4]Provided photons do not escape to infinity.

[5]In this paper we use irreversibility, for practical purposes, in part of the quantum mechanical algorithm.

[6]By restricting oneself to reversible algorithms, in principle heat production may be avoided altogether [15, 16].

understanding we write (1) as

$$|\Psi(t+\tau)\rangle = e^{i\hat{H}\tau/\hbar}|\Psi(t)\rangle. \tag{2}$$

In this way the *computational time* advances incrementally in unit steps of duration τ. Of course the state of the quantum computer exists at all intermediate times, say at $t+\frac{\tau}{2}$, but for our purposes we need only use the state at intervals of the time step τ. The quantum computer's evolution is invertible by application of the adjoint of the evolution operator

$$|\Psi(t-\tau)\rangle = e^{-i\hat{H}\tau/\hbar}|\Psi(t)\rangle. \tag{3}$$

This computational picture is consistent with the Heisenberg picture of quantum mechanics. For any reversible algorithm chosen, the task is to map the algorithm onto the dynamical evolution of interacting qubits of the physical device.

3 Quantum Lattice Gas

Lattice-gas quantum computation uses the superposition of multiple qubit states within a small spatial region of size ℓ only for a short amount of time on the order of the duration of a single time step, τ. A lattice-gas quantum computer has qubits arranged in a lattice-based array, with a small group of qubits at each site. Each site of the lattice can be thought of as a small quantum computer and all the quantum computers are connected in a lattice network. The quantum lattice gas' evolution can be formally expressed as a special case of (2) as follows

$$|\Psi(\vec{x}_1,\ldots,\vec{x}_V;t+\tau)\rangle = \hat{S}\hat{C}|\Psi(\vec{x}_1,\ldots,\vec{x}_V;t)\rangle, \tag{4}$$

where $\hat{S}$ is a unitary *streaming* matrix and $\hat{C}$ is a unitary *collision* matrix and where we have explicitly labeled the wavefunction's dependence on all the coordinates of the lattice. The operator $\hat{C}$ causes mixing of the outgoing collision configuration at each site of the lattice, locally entangling the qubit states within a lattice cell of radius size, ℓ. The operator $\hat{S}$ causes qubits to move from one site to the next, by exchanges between nearest neighboring sites (it is identical to its classical counterpart). Each qubit moves with unit speed, $c = \frac{\ell}{\tau}$, along one of the lattice directions, $\hat{e}_a$. Hence, in a completely coherent quantum computation, the application of $\hat{S}$ causes global entanglement of the all the qubit states[7]. It remains an intractable problem to theoretically analyze the dynamics of a quantum computer with many qubits because of the exponentially large size of the Hilbert space in which the entanglement occurs. And to make matters worse, even if a quantum computer was constructed with a large number of qubits, its wavefunction would decohere by uncontrolled entanglement with the external world and we know of no way to mitigate against this. So constructing

---

[7]Mathematically speaking, this is because both $\hat{S}$ and $\hat{C}$ cannot be simultaneously diagonalized

a large coherent quantum computer is difficult, if not all together impossible, and predicting its behavior by analytical means is intractable.

So what can be done about this? What I would like to consider is a simplification that will sidestep these obstacles and give us two important advantages: (1) a simple way to use a quantum computer with a large number of qubits; and (2) a way to analysis of its behavior. In lattice-gas quantum computation complete coherence of the wavefunction is not needed for the algorithm to work. In fact, we assume entanglement of qubit states is only among small clusters of qubits in a localized nearby neighborhood, so independent quantum operations are done in a classically parallel fashion on all sites simultaneously. This is the collision step.

In a deterministic classical lattice gas, the collision operator is a permutation matrix with components being either zero or one. In a probabilistic classical lattice gas, the collision operator is a transition matrix with real valued components. In contrast, in a quantum lattice gas, the collision operator can be a unitary matrix with complex components. The collision process is in general irreversible because a projection of the quantum computer's wavefunction into a tensor product state over the qubits is periodically made causing the wavefunction to partially collapse. Hence, application of $\hat{S}$ does not cause any global entanglement.

The quantum lattice gas presented here should not be confused with previous quantum lattice gas models by Succi [17], Boghosian [18], or Yepez [19] for simulating quantum mechanical systems. Despite some similarities, the type of quantum lattice gas treated in this paper is a direct generalization of a classical lattice gas with quantum bits replacing classical bits. In fact, if orthogonal permutation matrices with 0 and ± 1 components are used for the collision process, in the limit of complete collapse of the lattice-gas quantum computer's wavefunction, the quantum lattice gas exactly reduces to a classical lattice gas. This particular feature distinguishes the quantum lattice gas for fluid simulation from the quantum lattice gases for quantum mechanical simulation.

4 Preliminaries

Consider a lattice-gas quantum computer with the following properties:

- V is the number of lattice sites

- B is the number of qubits per site (and the number of nearest neighbors)

- $N = VB$ is the total number of qubits

- 2^N is the size of the full Hilbert space

- 2^B is the size of the on-site submanifold, denoted $\mathcal{H}$

- B is the size of the reduced on-site submanifold, denoted $\mathcal{B}$

We will use the following convention for indices:

Constants	Names
ℓ	length unit
τ	time unit
m	mass unit
c	velocity unit ($\frac{\ell}{\tau}$)
D	spatial dimension
B	lattice coordination number
e_{ai}	unit lattice vectors
a	directional index (1,2,..., B)
i,j,k,l	spatial indices

Table 1: Model Constants

Table 2: Wavefunction Symbols

Symbol	Size of Manifold	Description
Ψ	2^N	Total system wavefunction
ψ	2^B	On-site ket
ω	B	Partially collapsed on-site amplitudes
q	2	Qubit ket

- Small roman letters (a, b, c) for the $\mathcal{B}$-space dimensions, $a \in \{1, \ldots, B\}$

- Greek letters (α, β, γ) for the $\mathcal{H}$-space dimensions, $\alpha \in \{0, \ldots, 2^B - 1\}$

- Middle roman letters (i, j, k) for the spatial dimensions, $i \in \{1, \ldots, D\}$

The full Hilbert space of size 2^{BV} is partitioned into V independent quantum manifolds of dimension 2^B, as depicted in Fig.1. Quantum superposition of states occurs only within each 2^B-dimensional subspace, denoted $\mathcal{H}$. A general *on-site ket* defined over the basis states of $\mathcal{H}$ is the following

$$| \psi(\vec{x}, t)\rangle = \sum_{\alpha=0}^{2^B-1} \psi_\alpha(\vec{x}, t) \, | \, \alpha \rangle = \begin{pmatrix} \psi_0 \\ \psi_1 \\ \vdots \\ \psi_{2^B-1} \end{pmatrix}. \tag{5}$$

The ket $| \, \psi \rangle$ is specified by 2^B complex amplitudes, denoted $\psi_0, \ldots, \psi_{2^B-1}$. The quantum computer's total wavefunction is formed as a tensor product over all the $\mathcal{H}$-manifolds

$$| \Psi(\vec{x}_1, \ldots, \vec{x}_V; t)\rangle = \bigotimes_{x=1}^{V} | \, \psi(\vec{x}, t)\rangle. \tag{6}$$

The collision operator, $\hat{C}$, is blocked over all the $\mathcal{H}$-manifolds. That is, the collision matrix is block diagonal with V blocks each of size $2^B \times 2^B$, and

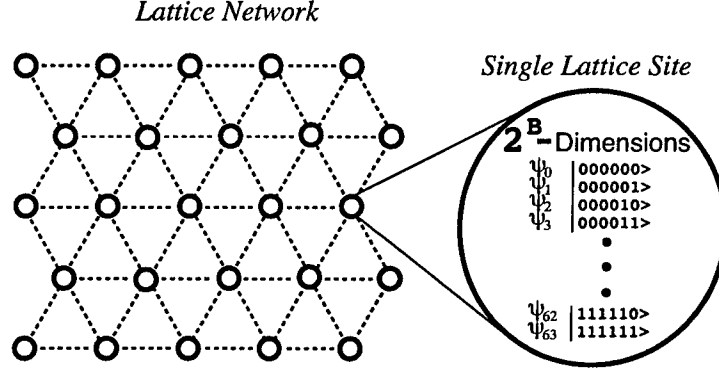*Lattice Network*

Figure 1: An array of small quantum computers (the quantum computers are depicted as circles) arranged in a 2-dimensional triangular lattice (B=6). The large circle on the right is an expanded view of a single quantum computer, which is one site of the lattice. It depicts the on-site submanifold, $\mathcal{H}$. Each quantum computer at a lattice node has 6 qubits so the on-site ket $| \psi \rangle$ resides in a 64-dimensional Hilbert space. Each node is coupled to its 6 nearest neighboring quantum computers by a mechanism allowing for the exchange of a single qubit.

therefore can be written as a tensor product

$$\hat{C} = \bigotimes_{x=1}^{V} \hat{U}. \tag{7}$$

The *on-site collision matrix*, $\hat{U}$, is unitary and acts on the on-site ket

$$| \psi'(\vec{x}, t) \rangle = \hat{U} | \psi(\vec{x}, t) \rangle. \tag{8}$$

The prime on the L.H.S. of (8) indicates that the ket is an *outgoing* collisional state.

5 Unitary Collision Matrix

Let $\hat{Q}_\alpha$ be matrices representing the conserved quantities in the single speed quantum lattice gas, $\hat{Q}_\alpha = (\hat{Q}_o, \hat{Q}_i)$ where i is an index over the independent spatial coordinates. A fundamental property of a quantum lattice gas is that the mass density and the momentum density can be written as follows

$$\rho = \langle \psi | \hat{Q}_o | \psi \rangle \tag{9}$$
$$\rho v_i = \langle \psi | \hat{Q}_i | \psi \rangle, \tag{10}$$

that is, where the component of $\hat{Q}_o$ are

$$(\hat{Q}_o)_{\mu\nu} \equiv m \delta_{\mu\nu} \sum_{a=1}^{B} b_{\mu a}, \tag{11}$$

7

and where the component of $\hat{Q}_i$ are

$$(\hat{Q}_i)_{\mu\nu} \equiv mc\delta_{\mu\nu} \sum_{a=1}^{B} b_{\mu a} e_{ai}. \tag{12}$$

The $b_{\mu a}$ denotes the ath-bit of the μth ket. The $\hat{e}_a$ here denote the unit lattice vectors where $a = 1, \ldots, B$. The components of the $2^B \times 2^B$ qubit number operator are defined by

$$(\hat{n}_a)_{\mu\nu} \equiv b_{\mu a}\delta_{\mu\nu}. \tag{13}$$

In terms of (13), the operators for mass and momentum are

$$\hat{Q}_\circ = m \sum_{a=1}^{B} \hat{n}_a \tag{14}$$

and

$$\hat{Q}_i = mc \sum_{a=1}^{B} e_{ai}\hat{n}_a. \tag{15}$$

In terms of (13) the invariant quantities are simply expressed as the following matrix elements

$$\rho = \sum_{a=1}^{B} m\langle \psi \mid \hat{n}_a \mid \psi \rangle \tag{16}$$

$$\rho v_i = \sum_{a=1}^{B} mce_{ai}\langle \psi \mid \hat{n}_a \mid \psi \rangle. \tag{17}$$

The matrix elements (9) and (10) must remain constant after each time step iteration

$$\langle \psi(t+\tau) \mid \hat{Q}_\alpha \mid \psi(t+\tau) \rangle = \langle \psi(t) \mid \hat{Q}_\alpha \mid \psi(t) \rangle. \tag{18}$$

Since $\mid \psi(t+\tau) \rangle = \hat{U} \mid \psi(t) \rangle$, this implies that

$$\hat{U}^\dagger \hat{Q}_\alpha \hat{U} = \hat{Q}_\alpha, \tag{19}$$

which is just the commutator

$$[\hat{U}, \hat{Q}_\alpha] = 0. \tag{20}$$

The matrices $\hat{Q}_\alpha$ must commute with $\hat{U}$.

Let $\hat{g}$ denote the generator of $\hat{U}$

$$\hat{U} = e^{i\varepsilon\hat{g}}, \tag{21}$$

where ε is an "Euler angle". Consider a "rotation" through an infinitesimal angle ε so that $\hat{U}$ can be Taylor expanded to first order as

$$\hat{U} = 1 + i\varepsilon\hat{g}. \tag{22}$$

The unitary condition, $\hat{U}^{\dagger}\hat{U} = 1$, implies that the generator is hermitian

$$\hat{g} - \hat{g}^{\dagger} = 0 + \mathcal{O}(\varepsilon^2). \tag{23}$$

From (19), we see that mass and momentum conservation is ensured provided

$$\hat{Q}_\alpha\hat{g} - \hat{g}^{\dagger}\hat{Q}_\alpha = 0 + \mathcal{O}(\varepsilon^2). \tag{24}$$

The solution of the set of linear equations (23) and (24) give the Lie algebra for the unitary group. Therefore, the mass density (9) and the momentum density (10) are conserved when each equivalence class block of the collision operator is an element of the unitary group $U(n)$ where n is the size of the equivalence class of the incoming local configuration. This is an important feature of a quantum lattice gas. Since any member of the unitary group can be used, the quantum lattice gas is algorithmically robust.
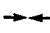

Figure 2: The equivalence classes for the quantum FHP lattice gas.

An *equivalence class* is defined as a set of basis states that correspond to particle configurations with the same mass and momentum. The unitary collision operator, $\hat{U}$, acting on the 2^B dimensional $\mathcal{H}$-manifold itself is block diagonal over the equivalence classes. For example, there are two equivalence classes for the FHP lattice gas [2], see Fig.2. The first equivalence class is comprised of the following two-body kets

$$|9\rangle = |001001\rangle$$
$$|18\rangle = |010010\rangle$$
$$|36\rangle = |100100\rangle$$

with mass, $m = 2$, and zero momentum, $\vec{p} = 0$. A general ket in this mass-momentum sector of the on-site manifold is a linear combination of these

$$\alpha|100100\rangle + \beta|010010\rangle + \gamma|001001\rangle, \tag{25}$$

where α, β, and γ are complex numbers. The second equivalence class is comprised of the following three-body kets

$$|21\rangle = |010101\rangle$$
$$|42\rangle = |101010\rangle$$

with mass, $m = 3$, and zero momentum, $\vec{p} = 0$. A general ket in this mass-momentum sector is a linear combination of these

$$\mu|101010\rangle + \nu|010101\rangle. \tag{26}$$

So $\hat{U}$ for a two-dimensional quantum lattice gas on a triangular lattice has two blocks, a $U(3)$ block for mixing the 2-body configurations and a $U(2)$ block for mixing the 3-body configurations.

For the triangular quantum lattice gas, we have

$$\begin{pmatrix} \psi'_{21} \\ \psi'_{42} \end{pmatrix} = e^{i\theta} \begin{pmatrix} e^{i\zeta}\cos\eta & e^{i\xi}\sin\eta \\ -e^{-i\xi}\sin\eta & e^{-i\zeta}\cos\eta \end{pmatrix} \begin{pmatrix} \psi_{21} \\ \psi_{42} \end{pmatrix}, \tag{27}$$

where zero momentum three-body configurations are mixed by a unitary matrix, $U(2) = U(1) \otimes SU(2)$, which in general has four free parameters. The zero momentum two-body configurations are mixed by a unitary matrix, $U(3) = U(1) \otimes SU(3)$, which in general has nine free paramters[8]

$$\begin{pmatrix} \psi'_9 \\ \psi'_{18} \\ \psi'_{36} \end{pmatrix} = e^{i\theta} SU(3) \begin{pmatrix} \psi_9 \\ \psi_{18} \\ \psi_{36} \end{pmatrix}. \tag{28}$$

6 Partial Collapse of Post-Collision Ket $|\psi'\rangle$

To avoid causing any global entanglement as induced by streaming, we project the post-collision ket $|\psi'\rangle$ which resides in the 2^B-dimensional $\mathcal{H}$ manifold onto a smaller B-dimensional submanifold, $\mathcal{B}$. This is done using a projection operator, denoted $\hat{\Gamma}$, as follows

$$|\omega'\rangle = \hat{\Gamma}|\psi'\rangle = \begin{pmatrix} \omega'_1 \\ \omega'_2 \\ \vdots \\ \omega'_B \end{pmatrix}. \tag{29}$$

The operator $\hat{\Gamma}$ causes a partial collapse of the locally entangled on-site state $|\psi\rangle$ resulting in a nonentangled state $|\omega\rangle$ residing in a smaller manifold (a mapping

---

[8]We do not write out the SU(3) matrix in component form because it is too complicated.

2^{B}-Dimensions　　　　　　　　　**B-Dimensions**

$$\begin{array}{ll}\psi_0 & |000000\rangle\\ \psi_1 & |000001\rangle\\ \psi_2 & |000010\rangle\\ \psi_3 & |000011\rangle\\ & \bullet\\ & \bullet\\ & \bullet\\ \psi_{62} & |111110\rangle\\ \psi_{63} & |111111\rangle\end{array}$$

Projection →

← **Injection**

$$\begin{array}{ll}\omega_1 & |1\rangle\\ \omega_2 & |2\rangle\\ \omega_3 & |3\rangle\\ \omega_4 & |4\rangle\\ \omega_5 & |5\rangle\\ \omega_6 & |6\rangle\end{array}$$
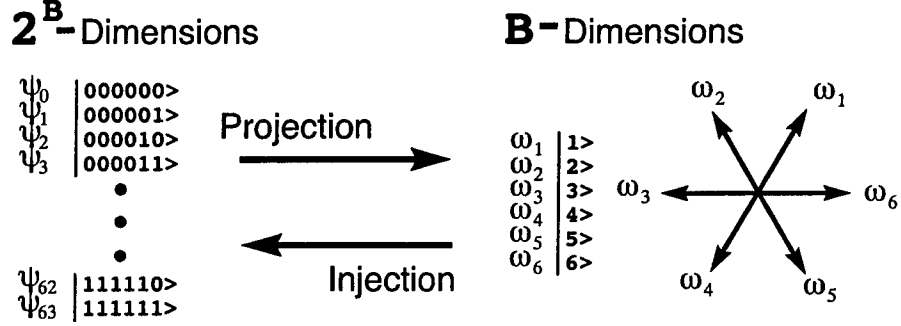

Figure 3: Two-dimensional quantum lattice gas on a triangular lattice. The lattice coordination number is $B = 6$. There are $2^6 = 64$ amplitudes in the $\mathcal{H}$-manifold and 6 amplitudes in the $\mathcal{B}$-manifold. *Injection* maps the 6 on-site amplitudes ω_a in the $\mathcal{B}$-manifold into the larger $\mathcal{H}$-manifold. The inverse process, *projection*, maps the 64 amplitudes ψ_α in the $\mathcal{H}$-manifold onto 6 amplitudes ω_a in the $\mathcal{B}$-manifold. The projection is a measurement process that causes a partial collapse of the on-site wavefunction $|\psi(\vec{x},t)\rangle$. The partially collapsed wavefunction is $|\omega(\vec{x},t)\rangle$.

from 64 dimensions down to 6, see Fig.3). Thus $|\omega\rangle$ in (29) may be termed the *collapsed post-collisional on-site ket*. By construction, the action of $\hat{\Gamma}$ fixes the phase, θ_a, of the on-site qubits $|q_a\rangle$ according to the following recipe

$$|q_a\rangle = \cos\theta_a\,|1\rangle + \sin\theta_a\,|0\rangle, \tag{30}$$

where $\omega_a = \cos\theta_a$. That is,

$$|q_a\rangle = \omega_a\,|1\rangle + \sqrt{1 - \omega_a^*\omega_a}\,|0\rangle. \tag{31}$$

After the collapse of the ket $|\psi\rangle$ the *single-particle occupation probability*, denoted f_a, is a well-defined quantity. It is the probability of finding a particle at coordinate $(\vec{x},t)$ with momentum $mc\hat{e}_a$

$$f_a(\vec{x},t) = \omega_a^*(\vec{x},t)\omega_a(\vec{x},t). \tag{32}$$

Using the single qubit number operator $\hat{n} = \begin{pmatrix} 1 & 0 \\ 0 & 0 \end{pmatrix}$, (32) can be written in terms of the qubit ket as

$$f_a(\vec{x},t) = \langle q_a(\vec{x},t)\,|\,\hat{n}\,|\,q_a(\vec{x},t)\rangle. \tag{33}$$

Furthermore, in (16) and (17), the matrix element $\langle\psi\,|\,\hat{n}_a\,|\,\psi\rangle$ also gives the probability of particle occupancy. So for a quantum lattice gas, f_a can also be expressed as the matrix element of the multiple qubit number operator[9]

$$f_a = \langle\psi\,|\,\hat{n}_a\,|\,\psi\rangle. \tag{34}$$

---

[9]In a classical lattice gas the single-particle occupation probability is obtained by ensemble averaging over the number variables, $f_a = \langle n_a\rangle$, where $n_a = 0$ or 1.

Inserting the expression for the outgoing collisional state (8) into the R.H.S. of (29), we have

$$| \, \omega' \rangle = \hat{\Gamma} \hat{U} \, | \, \psi \rangle. \tag{35}$$

In §7 we will use a nonlinear function for the projection operator. Our goal is to retain as much quantum information as possible while allowing (35) to reduce to the collision equation of classical lattice gas transport when $\hat{U}$ is a real-valued permutation matrix. This is accomplished by projecting down from the $\mathcal{H}$-manifold containing 2^B complex amplitudes to the $\mathcal{B}$-manifold with only B complex amplitudes. Each ω_a (or associated qubit $| \, q_a \rangle$) is "attached" to one of the lattice directions. The reason for this reduction of the quantum information is the following. By using only B complex amplitudes, one for each direction, we can straightforwardly write down a quasi-classical streaming equation in analogy to the streaming equation of a classical lattice gas

$$| \, \omega(\vec{x} + \ell \vec{\mathcal{L}}_a, t + \tau) \rangle = | \, \omega'(\vec{x}, t) \rangle, \tag{36}$$

where $\mathcal{L}_{abi} \equiv \hat{e}_{ai} \delta_{ab}$. Inserting (35) into (36), we have

$$| \, \omega(\vec{x} + \ell \vec{\mathcal{L}}_a, t + \tau) \rangle = \hat{\Gamma} \hat{U} \, | \, \psi(\vec{x}, t) \rangle. \tag{37}$$

The only task remaining to complete the analogy to classical lattice gas dynamics is to rewrite the R.H.S. of (37) solely in terms of the ω's. This can be done by *injecting* the on-site collapsed ket $| \, \omega \rangle$ residing in the sub-manifold $\mathcal{B}$ up into the larger on-site manifold $\mathcal{H}$ (see Fig.3). This process can be expressed by application of an *injection operator*, $\hat{I}$, as follows

$$| \, \psi(\vec{x}, t) \rangle = \hat{I} \, | \, \omega(\vec{x}, t) \rangle. \tag{38}$$

A straightforward way to accomplish the injection is to take the tensor product over the on-site qubits

$$| \, \psi(\vec{x}, t) \rangle = \bigotimes_{a=1}^{B} | \, q_a(\vec{x}, t) \rangle. \tag{39}$$

This is a nonlinear operation.[10] Let us revisit the example a two-dimensional quantum lattice gas on a triangular lattice ($B = 6$), a generalization of the classical FHP lattice gas [2]. Fig.3 illustrates projection from the 64-dimensional $\mathcal{H}$-manifold down to the 6-dimensional $\mathcal{B}$-manifold and illustrates injection from the $\mathcal{B}$-manifold up to the $\mathcal{H}$-manifold. The 6 on-site amplitudes ω_a (or the associated 6 on-site qubits $| \, q_a \rangle$) generated by the projection can be streamed in a classical fashion. After streaming to their new sites, each quantum computer has a new incoming configuration of the ω_a amplitudes. Before this configuration can be collided, they must be injected up to the larger 64-dimensional manifold where the collision process is well defined.

---

[10]A non-square linear matrix could also be used, but it is difficult to find an appropriate matrix even though it can be shown that one exists.

Inserting (38) into (35) gives

$$| \omega'(\vec{x}, t) \rangle = \hat{\Gamma} \hat{U} \hat{I} | \omega(\vec{x}, t) \rangle. \tag{40}$$

Using the fact that the projection of the injection is the identity operation: $| \omega \rangle \equiv \hat{\Gamma} \hat{I} | \omega \rangle$, we write (40) in a form analogous to the classical lattice gas collision equation

$$| \omega'(\vec{x}, t) \rangle = | \omega(\vec{x}, t) \rangle + \left[\hat{\Gamma} \hat{U} \hat{I} | \omega(\vec{x}, t) \rangle - \hat{\Gamma} \hat{I} | \omega(\vec{x}, t) \rangle \right]. \tag{41}$$

Finally, we arrive at the quantum lattice gas microscopic transport equation by inserting (41) into (36)

$$| \omega(\vec{x} + \ell \vec{\hat{\mathcal{L}}}_a, t + \tau) \rangle = | \omega(\vec{x}, t) \rangle + | \Omega(\vec{x}, t) \rangle, \tag{42}$$

where the quantum lattice gas collision operator is defined as

$$| \Omega(\vec{x}, t) \rangle \equiv \hat{\Gamma} \hat{U} \hat{I} | \omega(\vec{x}, t) \rangle - \hat{\Gamma} \hat{I} | \omega(\vec{x}, t) \rangle. \tag{43}$$

In component form, (42) is

$$\omega_a(\vec{x} + \ell \hat{e}_a, t + \tau) = \omega_a(\vec{x}, t) + \Omega_a\left(\omega_*(\vec{x}, t) \right). \tag{44}$$

Equation (44) is identical in form to the classical lattice gas transport equation where the occupation variable, $n_a = 0$ or 1, is replaced by a complex amplitude, $0 \leq |\omega_a| \leq 1$, that continuously encodes the square root of the probability for particle occupancy. Hence (44) is a much more useful expression of the quantum lattice gas dynamics than (4) is.

7 The Projection Operator

We can write an analytical expression for the projection operator where the amplitudes ω_a a nonlinear function of the amplitudes ψ_a

$$\omega_a = \hat{\Gamma}_a(\psi) \equiv \sqrt{\sum_{\alpha=0}^{2^B-1} |\psi_\alpha|^2 \, b_{\alpha a}}. \tag{45}$$

Note that $b_{\alpha a} = 0$ or 1 is the Boolean value of the ath bit of the αth ket in the number representation. Let $\hat{m}$ and $\hat{p}_i$ be the operators for mass and momentum in the $\mathcal{B}$-space. Then the matrix element for the mass density is

$$\rho = \langle \omega | \hat{m} | \omega \rangle, \tag{46}$$

where $\hat{m}_{ab} = m \delta_{ab}$, and the matrix element for the momentum density is

$$\rho v_i = \langle \omega | \hat{p}_i | \omega \rangle, \tag{47}$$

13

where $(\hat{p}_i)_{ab} = mce_{ai}\delta_{ab}$. $\hat{Q}_o$ and $\hat{Q}_i$ were defined in §5 to be the mass and momentum operators in ψ-space. Here we have mass and momentum operators in ω-space. The matrix element (9) defines the mass density as $\rho = \langle \psi \mid \hat{Q}_o \mid \psi \rangle$, where $(\hat{Q}_o)_{\alpha\beta} = m \sum_{a=1}^{B} b_{a\alpha}\delta_{\alpha\beta}$, and the matrix element (10) defines the momentum density as $\rho v_i = \langle \psi \mid \hat{Q}_i \mid \psi \rangle$, where $(\hat{Q}_i)_{\alpha\beta} = mc \sum_{a=1}^{B} b_{a\alpha}e_{ai}\delta_{ab}$. Equating (46) with (9) and equating (47) with (10) gives us a way to check the projection operator (45).

This is done as follows

$$\langle \omega \mid \hat{m} \mid \omega \rangle = m \sum_{a=1}^{B} \mid \omega_a \mid^2 \tag{48}$$

$$= m \sum_{a=1}^{B} \sum_{\alpha=1}^{2^B} \mid \psi_\alpha \mid^2 b_{\alpha a} \tag{49}$$

$$= \sum_{\alpha=1}^{2^B} \mid \psi_\alpha \mid^2 \left(m \sum_{a=1}^{B} b_{\alpha a} \right), \tag{50}$$

where we used the square of (45) on the second line of the derivation. Therefore, we have

$$\langle \omega \mid \hat{m} \mid \omega \rangle = \langle \psi \mid \hat{Q}_o \mid \psi \rangle, \tag{51}$$

where the mass operator in ψ-space

$$(\hat{Q}_o)_{\alpha\beta} = m \sum_{a=1}^{B} b_{\alpha a}\delta_{\alpha\beta} \tag{52}$$

is identical to $\hat{Q}_o$ defined in (9). So the projection operator (45) conserves mass. We continue the consistency check by rewriting (47)

$$\langle \omega \mid \hat{p}_i \mid \omega \rangle = mc \sum_{a=1}^{B} \mid \omega_a \mid^2 e_{ai} \tag{53}$$

$$= mc \sum_{a=1}^{B} \sum_{\alpha=1}^{2^B} \mid \psi_\alpha \mid^2 b_{\alpha a}e_{ai} \tag{54}$$

$$= \sum_{\alpha=1}^{2^B} \mid \psi_\alpha \mid^2 \left(mc \sum_{a=1}^{B} b_{\alpha a}e_{ai} \right), \tag{55}$$

where again we used the square of (45) on the second line of the derivation. Therefore, we have

$$\langle \omega \mid \hat{p}_i \mid \omega \rangle = \langle \psi \mid \hat{Q}_i \mid \psi \rangle, \tag{56}$$

where the momentum operator in ψ-space

$$(\hat{Q}_i)_{\alpha\beta} = mc \sum_{a=1}^{B} b_{\alpha a}e_{ai}\delta_{\alpha\beta}, \tag{57}$$

14

is identical to $\hat{Q}_i$ defined in (10). So the projection operator (45) conserves momentum as well as mass.

8 Equilibrium Ansatz

The ω_a amplitudes in $\mathcal{B}$-space can be ordered in powers of ε as follows

$$| \omega \rangle = | \omega^{(0)} \rangle + \varepsilon | \omega^{(1)} \rangle + \mathcal{O}(\varepsilon^2), \tag{58}$$

where $| \omega^{(0)} \rangle$ denotes the *equilibrium ket* and where the ket $| \omega^{(1)} \rangle$ is the first order correction from equilibrium. The condition equilibrium is that $| \omega^{(0)} \rangle$ satisfies the following identity

$$| \omega^{(0)} \rangle = \hat{\Gamma} \hat{U} \hat{I} | \omega^{(0)} \rangle. \tag{59}$$

Note that the associated equilibrium ket in $\mathcal{H}$-space, $| \psi^{(0)} \rangle$, follows from (58) by injection $| \psi \rangle = \hat{I} | \omega \rangle$

$$| \psi \rangle = | \psi^{(0)} \rangle + \varepsilon | \psi^{(1)} \rangle + \mathcal{O}(\varepsilon^2). \tag{60}$$

So we can also write (59) as follows

$$| \psi^{(0)} \rangle = \hat{U} | \psi^{(0)} \rangle. \tag{61}$$

It is clear that $| \psi^{(0)} \rangle$ is an eigenvector of $\hat{U}$ with unity eigenvalue. Using (59), we immediately see that the collision operator (43) vanishes at equilibrium

$$| \Omega(\omega^{(0)}) \rangle = \hat{\Gamma} \hat{U} \hat{I} | \omega^{(0)} \rangle - \hat{\Gamma} \hat{I} | \omega^{(0)} \rangle = 0. \tag{62}$$

Equations (58) and (59) constitute the essential ansatz that will allow us to perform a Chapman-Enskog analysis of the quantum lattice gas. It is possible to analytically solve (59) for $| \omega^{(0)} \rangle$. Knowing the form of $| \omega^{(0)} \rangle$, we can predict the hydrodynamics equations of the quantum lattice gas at the macroscopic scale. In the Chapman-Enskog analysis, we expand the collision operator, $| \Omega \rangle$, about this equilibrium ket $| \omega^{(0)} \rangle$. In so doing, the Jacobian of the collision operator is computed as a first order correction and is evaluated at $| \omega \rangle = | \omega^{(0)} \rangle$. The transport coefficients for the mass diffusion, shear viscosity, and bulk viscosity depend on the value of this first order correction, and this in turn depends on the value of $| \omega^{(0)} \rangle$. Hence, one must determine the equilibrium amplitudes in order to compute the value of the transport coefficients.

The a single particle occupancy probability $f_a = \omega_a^{*(0)} \omega_a^{(0)} = \langle q_a^{(0)} | \hat{n} | q_a^{(0)} \rangle = \langle \psi | \hat{n}_a | \psi \rangle$ has the functional form

$$f_a = \frac{1}{e^{\alpha \rho + \beta \hat{\varepsilon}_a \cdot \vec{p} + \gamma E} + 1}, \tag{63}$$

where the argument of the exponential is a linear combination of the conserved scalar quantities: (1) the mass ρ; (2) the momentum component $\hat{e}_a \cdot \vec{p}$ along
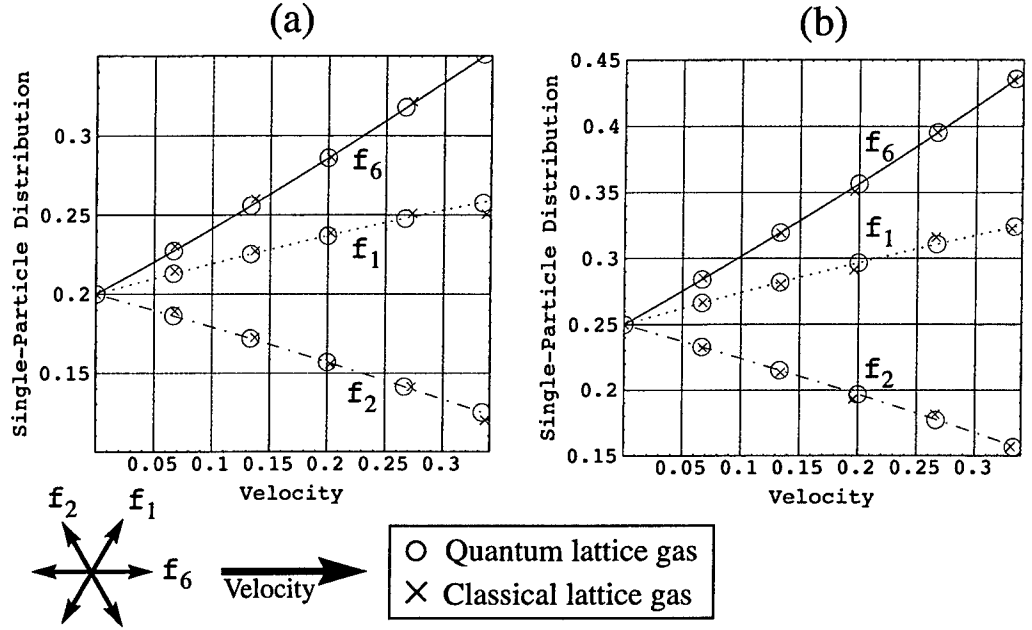
15

Figure 4: Theory versus simulation comparison of the velocity dependence of the single-particle distribution function in the non-Galilean parameterization: $f_a = \omega_a^* \omega_a = d + dD\hat{e}_a \cdot \vec{v} + gdD(D/2 + 1)\hat{Q}_a : \vec{v}\vec{v}$. FHP simulation data is overplotted on this predicted mesoscopic distribution function. Plots (a) and (b) are for background densities of $d = .20$ and $d = 0.25$, respectively. A velocity shift is imparted along the x-axis; that is, along the f_1 direction indicated in the figure. Data was collected from a 128×128 classical FHP simulation (crosses) and was coarse-grained averaged over 1600 time steps from time step $t = 400$ to $t = 2000$. Data was also collected from a smaller 32×32 quantum FHP simulation (circles) and were measured at a single time step at $t = 200$.

the lattice direction $\hat{e}_a$; and (3) the energy E at a lattice site. The real valued coefficients α, β, and γ are free parameters that are fixed by the non-Galilean parameterization given in Appendix A. The reason for the form of (63) is the collision matrix $\hat{U}$ is unitary and so the collisions obey detailed balance.

In the quantum limit, where the quantum lattice gas becomes a fully coherent quantum system that undergoes unitary evolution, we expect the equilibrium probability for the particle occupancy to have the form of (63). In the opposite limit, the classical limit, where there is a complete collapse of the ket $| \Psi \rangle$ everywhere, the quantum lattice gas reduces to a classical lattice gas system. In the classical limit too, the particle occupancies are described by (63). Our quantum lattice gas dynamics is somewhere midway between a fully quantum system and a fully classical system. Since both ends of the spectrum are described by (63), it is not altogether unexpected that the middle regime is too.

However, this is not obvious. At first glance, it appears that the destructive act of projecting from the $\mathcal{H}$-manifold onto the $\mathcal{B}$-manifold might destroy the form of the equilibrium distribution. But it does not (see Fig.4); the distribution (63) describes the particle occupancy of our quantum lattice gas [3]. Taking $\omega_a = \sqrt{\langle q_a^{(0)} \mid \hat{n} \mid q_a^{(0)} \rangle}$, the result (see Appendix A) is the following[11]

$$\mid \omega \rangle = \sqrt{d} \left(\mid \mathbf{1} \rangle + \frac{D}{2c} \vec{v} \cdot \mid \hat{e} \rangle + \frac{gD(D+2)}{4c^2} \vec{v}\vec{v} : \mid Q \rangle \right), \tag{64}$$

where

$$\mid \mathbf{1} \rangle \equiv \begin{pmatrix} 1 \\ 1 \\ 1 \\ 1 \\ 1 \\ 1 \end{pmatrix} \tag{65}$$

$$\mid \hat{e} \rangle \equiv \hat{\mathcal{L}} \mid \mathbf{1} \rangle, \tag{66}$$

and

$$\mid Q \rangle \equiv (\hat{\mathcal{L}}\hat{\mathcal{L}} - \frac{1}{D}) \mid \mathbf{1} \rangle. \tag{67}$$

Taylor expanding the collision operator gives

$$\Omega_a(\omega) = \Omega_a\left(\omega^{(0)}\right) + \varepsilon \frac{\partial \Omega_a(\omega)}{\partial \omega_b} \bigg|_{\omega=\omega^{(0)}} \omega_b^{(1)} + \mathcal{O}(\varepsilon^2). \tag{68}$$

Using the equilibrium condition (62), the first term on the R.H.S. vanishes and we are left with

$$\Omega_a(\omega) = \varepsilon \mathcal{J}_{ab} \omega_b^{(1)} + \mathcal{O}(\varepsilon^2), \tag{69}$$

where the Jacobian of the projection operator is defined as

$$\mathcal{J}_{ab} \equiv \frac{\partial \Omega_a(\omega)}{\partial \omega_b} \bigg|_{\omega=\omega^{(0)}}. \tag{70}$$

Equation (69) can be written in vector form as

$$\mid \hat{\Omega}(\omega) \rangle = \varepsilon \mathcal{J} \mid \omega^{(1)} \rangle + \mathcal{O}(\varepsilon^2). \tag{71}$$

9 Boltzmann Equation for the Quantum Lattice Gas

The quantum lattice gas microscopic transport equation (42) is

$$\mid \omega(\vec{x}\mathbf{1} + \varepsilon \ell \vec{\hat{\mathcal{L}}}, t + \varepsilon^2 \tau) \rangle = \mid \omega(\vec{x}, t) \rangle + \mid \Omega(\vec{x}, t) \rangle.$$

[11]In (64), we have used the approximation $\sqrt{1+x} \cong 1 + \frac{x}{2}$, which holds for small x.

Near equilbrium, each application of the projection operator causes only small changes in the phase of $\mid \omega \rangle$ allowing us to Taylor expand the L.H.S. of (42). Taylor expanding (42) to second order in ε gives a Boltzmann equation

$$\varepsilon^2 \partial_t \mid \omega(\vec{x}, t) \rangle + \left(\varepsilon c \hat{\mathcal{L}}_i \partial_i + \frac{\varepsilon^2 \ell^2}{2\tau} \hat{\mathcal{L}}_i \hat{\mathcal{L}}_j \partial_i \partial_j \right) \mid \omega(\vec{x}, t) \rangle + \mathcal{O}(\varepsilon^3) = \frac{1}{\tau} \mid \Omega(\vec{x}, t) \rangle. \tag{72}$$

In analogy with a classical lattice, we impose two constraints on the collision operator regarding the isometries of the lattice. The first constraint is

$$\langle \omega \mid \hat{m} \mid \Omega \rangle = 0, \tag{73}$$

and this will be needed when we take the zeroth moment of (72). This constraint enforces mass conservation. The second constraint to enforce momentum conservation is

$$\langle \omega \mid \hat{p}_i \mid \Omega \rangle = 0, \tag{74}$$

and this will be needed when we take the first moment of (72). Inserting the ε-expansion of $\mid \omega_a \rangle$, (58), and the ε-expansion of $\mid \Omega_a \rangle$, (71), into the quantum lattice gas transport equation, (72), and keeping terms up to second order in ε gives

$$\varepsilon^2 \partial_t \mid \omega^{(0)} \rangle + \frac{\varepsilon}{\tau} \hat{\mathcal{L}}_i \partial_i \mid \omega^{(0)} \rangle + \frac{\varepsilon^2}{\tau} \hat{\mathcal{L}}_i \partial_i \mid \omega^{(1)} \rangle + \frac{\varepsilon^2}{2\tau} \hat{\mathcal{L}}_i \hat{\mathcal{L}}_j \partial_i \partial_j \mid \omega^{(0)} \rangle = \frac{\varepsilon}{\tau} \mathcal{J} \mid \omega^{(1)} \rangle + \mathcal{O}(\varepsilon^3). \tag{75}$$

Now equating the order-ε terms, we get

$$\hat{\mathcal{J}} \mid \omega^{(1)} \rangle = \hat{\mathcal{L}}_i \partial_i \mid \omega^{(0)} \rangle. \tag{76}$$

Then inverting the kinetic part of the Jacobian matrix gives

$$\mid \omega^{(1)} \rangle = \ell \hat{\mathcal{J}}^{-1} \left(\omega^{(0)} \right) \hat{\mathcal{L}}_i \partial_i \mid \omega^{(0)} \rangle. \tag{77}$$

So the first order correction ket is equated to the gradient of the equilibrium ket. Inserting this result back into (58) we have

$$\mid \omega \rangle = \mid \omega^{(0)} \rangle + \varepsilon \hat{\mathcal{J}}^{-1} \hat{\mathcal{L}}_i \partial_i \mid \omega^{(0)} \rangle + \mathcal{O}(\varepsilon^2), \tag{78}$$

Inserting (64) into (78), we have the subsonic ε-expansion of $\mid \omega \rangle$ good to first order in ϵ

$$\mid \omega \rangle = \sqrt{d} \left(\mid 1 \rangle + \frac{D}{2c} \vec{v} \cdot \mid \hat{e} \rangle + \frac{gD(D+2)}{4c^2} \vec{v}\vec{v} : \mid Q \rangle + \frac{\varepsilon D}{2c} \hat{\mathcal{J}}^{-1} \hat{\mathcal{L}} \hat{\mathcal{L}} : \nabla \vec{v} \mid 1 \rangle \right) + \mathcal{O}(\varepsilon^2). \tag{79}$$

10 Hydrodynamic Equations

ZEROTH MOMENT EQUATION:

Now we can write the *zeroth moment* of the Boltzmann equation (72) by left multiplying by $\langle\omega|\hat{m}$ as follows

$$\varepsilon^2\langle\omega\mid\hat{m}\mid\partial_t\omega\rangle + \varepsilon\langle\omega\mid\hat{m}c\hat{\mathcal{L}}_i\mid\partial_i\omega\rangle + \frac{\varepsilon^2\ell^2}{2\tau}\langle\omega\mid\hat{m}\hat{\mathcal{L}}_i\hat{\mathcal{L}}_j\mid\partial_i\partial_j\omega\rangle = \frac{1}{\tau}\langle\omega\mid\hat{m}\mid\Omega\rangle. \tag{80}$$

The adjoint of (80) is the following

$$\varepsilon^2\langle\partial_t\omega\mid\hat{m}\mid\omega\rangle + \varepsilon\langle\partial_i\omega\mid\hat{\mathcal{L}}_i\hat{m}c\mid\omega\rangle + \frac{\varepsilon^2\ell^2}{2\tau}\langle\partial_i\partial_j\omega\mid\hat{\mathcal{L}}_i\hat{\mathcal{L}}_j\hat{m}\mid\omega\rangle = \frac{1}{\tau}\langle\Omega\mid\hat{m}\mid\omega\rangle, \tag{81}$$

and the R.H.S. will also vanishes because of constraint (73). Because $\hat{m}$ and $\mathcal{L}$ commute, adding (80) and (81) gives us the following zeroth moment equation

$$\varepsilon^2\partial_t\langle\omega\mid\hat{m}\mid\omega\rangle + \varepsilon\partial_i\langle\omega\mid\hat{m}c\hat{\mathcal{L}}_i\mid\omega\rangle + \frac{\varepsilon^2\ell^2}{2\tau}\left(\langle\omega\mid\hat{m}\hat{\mathcal{L}}_i\hat{\mathcal{L}}_j\mid\partial_i\partial_j\omega\rangle + \langle\partial_i\partial_j\omega\mid\hat{\mathcal{L}}_i\hat{\mathcal{L}}_j\hat{m}\mid\omega\rangle\right) = 0. \tag{82}$$

FIRST MOMENT EQUATION:

Now we can write the *first moment* of (72) by left multiplying by $\langle\omega|\hat{p}_i$ as follows

$$\varepsilon^2\langle\omega\mid\hat{p}_i\mid\partial_t\omega\rangle + \varepsilon\langle\omega\mid\hat{p}_ic\hat{\mathcal{L}}_j\mid\partial_j\omega\rangle + \frac{\varepsilon^2\ell^2}{2\tau}\langle\omega\mid\hat{p}_i\hat{\mathcal{L}}_j\hat{\mathcal{L}}_k\mid\partial_j\partial_k\omega\rangle = 0, \tag{83}$$

where the R.H.S. vanishes because of the second constraint (74) on the collision operator. Because $\hat{p}$ and $\mathcal{L}$ commute, adding (83) to its adjoint equation gives us the following first moment equation

$$\varepsilon^2\partial_t\langle\omega\mid\hat{p}_i\mid\omega\rangle + \varepsilon\partial_j\langle\omega\mid\hat{p}_ic\hat{\mathcal{L}}_j\mid\omega\rangle + \frac{\varepsilon^2\ell^2}{2\tau}\left(\langle\omega\mid\hat{p}_i\hat{\mathcal{L}}_j\hat{\mathcal{L}}_k\mid\partial_j\partial_k\omega\rangle + \langle\partial_k\partial_j\omega\mid\hat{\mathcal{L}}_k\hat{\mathcal{L}}_j\hat{p}_i\mid\omega\rangle\right) = 0. \tag{84}$$

The zeroth and first momentum equations (82) and (84) are partial differential equations in the matrix elements. The macroscopic equations of motion, a mass continuity equation and a Navier-Stokes equation, come from (82) and (84), respectively.

We can now determine the partial differential equations that describe the dynamics of a quantum lattice gas in local equilibrium. Inserting (78) into the zeroth moment equation (82) and retaining terms up to second order in the smallness gives

$$\varepsilon^2\partial_t\left(m\langle\omega^{(0)}\mid\omega^{(0)}\rangle\right) \quad + \quad \varepsilon\partial_i\left(mc\langle\omega^{(0)}\mid\hat{\mathcal{L}}_i\mid\omega^{(0)}\rangle\right) = \tag{85}$$

$$-\frac{m\varepsilon^2\ell^2}{\tau}\partial_i\left(\langle\omega^{(0)}\mid\hat{\mathcal{L}}_i\hat{\mathcal{J}}^{-1}\hat{\mathcal{L}}_j\mid\partial_j\omega^{(0)}\rangle + \langle\partial_j\omega^{(0)}\mid\hat{\mathcal{L}}_j(\hat{\mathcal{J}}^{-1})^*\hat{\mathcal{L}}_i\mid\omega^{(0)}\rangle\right)$$

$$-\frac{m\varepsilon^2\ell^2}{2\tau}\left(\langle\omega^{(0)}\mid\hat{\mathcal{L}}_i\hat{\mathcal{L}}_j\mid\partial_i\partial_j\omega^{(0)}\rangle + \langle\partial_i\partial_j\omega^{(0)}\mid\hat{\mathcal{L}}_i\hat{\mathcal{L}}_j\mid\omega^{(0)}\rangle\right),$$

19

using the fact that $\hat{m} = m\mathbf{1}$. Identifying the local equilibrium mass density (46), $\rho = m\langle \omega^{(0)} \mid \omega^{(0)} \rangle$, and momentum density (47), $\rho v_i = mc\langle \omega^{(0)} \mid \hat{\mathcal{L}}_i \mid \omega^{(0)} \rangle$, we arrive at the hydrodynamic equation for mass flow

$$
\varepsilon^2 \partial_t \rho \;+\; \varepsilon \partial_i (\rho v_i) = \tag{86}
$$
$$
-\; \frac{m\varepsilon^2 \ell^2}{\tau} \partial_i \left(\langle \omega^{(0)} \mid \hat{\mathcal{L}}_i \hat{\mathcal{J}}^{-1} \hat{\mathcal{L}}_j \mid \partial_j \omega^{(0)} \rangle + \langle \partial_j \omega^{(0)} \mid \hat{\mathcal{L}}_j (\hat{\mathcal{J}}^{-1})^* \hat{\mathcal{L}}_i \mid \omega^{(0)} \rangle \right)
$$
$$
-\; \frac{m\varepsilon^2 \ell^2}{2\tau} \left(\langle \omega^{(0)} \mid \hat{\mathcal{L}}_i \hat{\mathcal{L}}_j \mid \partial_i \partial_j \omega^{(0)} \rangle + \langle \partial_i \partial_j \omega^{(0)} \mid \hat{\mathcal{L}}_i \hat{\mathcal{L}}_j \mid \omega^{(0)} \rangle \right),
$$

Similarly, by inserting (78) into the first moment equation (84) and retaining terms up to second order in the smallness gives the hydrodynamic equation for momentum flow

$$
\varepsilon^2 \partial_t (\rho v_i) \;+\; \varepsilon \partial_j \Pi_{ij}^{\text{ideal}} = \tag{87}
$$
$$
-\; \varepsilon^2 mc^2 \ell \partial_j \left(\langle \omega^{(0)} \mid \hat{\mathcal{L}}_i \hat{\mathcal{L}}_j \hat{\mathcal{J}}^{-1} \hat{\mathcal{L}}_k \mid \partial_k \omega^{(0)} \rangle + \langle \partial_k \omega^{(0)} \mid \hat{\mathcal{L}}_k (\hat{\mathcal{J}}^{-1})^* \hat{\mathcal{L}}_j \hat{\mathcal{L}}_i \mid \omega^{(0)} \rangle \right)
$$
$$
-\; \frac{\varepsilon^2}{2} mc^2 \ell \left(\langle \omega^{(0)} \mid \hat{\mathcal{L}}_i \hat{\mathcal{L}}_j \hat{\mathcal{L}}_k \mid \partial_j \partial_k \omega^{(0)} \rangle + \langle \partial_k \partial_j \omega^{(0)} \mid \hat{\mathcal{L}}_k \hat{\mathcal{L}}_j \hat{\mathcal{L}}_i \mid \omega^{(0)} \rangle \right),
$$

where the ideal part of the momentum flux density tensor is defined as

$$
\Pi_{ij}^{\text{ideal}} \equiv mc^2 \langle \omega^{(0)} \mid \hat{\mathcal{L}}_i \hat{\mathcal{L}}_j \mid \omega^{(0)} \rangle. \tag{88}
$$

To obtain the macroscopic equations of motion, we have to determine the value of the matrix elements appearing in (86), (87) and (88). This is carried out in Appendix B. The result is that in the incompressible limit ($\nabla \cdot \vec{v} = 0$), all the matrix elements on the R.H.S. of (86) vanish leaving us with a mass continuity equation

$$
\partial_t \rho + \partial_i (\rho v_i) = 0, \tag{89}
$$

and the matrix elements on the R.H.S. of (87) do not vanish leaving us with a viscous Navier-Stokes equation[12]

$$
\partial_t (\rho v_i) + \partial_g (g \rho v_i v_j) = -\partial_i P + \rho \nu \partial^2 v_i. \tag{90}
$$

In (90), the pressure is

$$
P = \rho \frac{c^2}{D} \left(1 - g\frac{v^2}{c^2} \right), \tag{91}
$$

and the kinematic shear viscosity is

$$
\nu = \frac{\ell^2}{\tau(D+2)} \left(\frac{1}{\kappa_\eta} - \frac{1}{2} \right). \tag{92}
$$

The form of the kinematic viscosity (92) is identical to that for the classical lattice gas as found by Henon [20]. However, in the case of the quantum lattice gas, the value of κ_η can be different than the classical value because of quantum mechanical interference of outgoing collision possibilities.

---

[12] As is the case for the classical lattice gas, there is a density dependent prefactor appearing in the convective term and the pressure, $g(d) = \frac{D}{D+2} \frac{1-2d}{1-d}$.

11 Summary

In this paper, we predicted the macroscopic behavior of a lattice-gas quantum computer. The following observations are made:

1. The Ψ-space unitary collision matrix, $\hat{C}$, is successively blocked, first over the on-site 2^B-dimensional manifold, $\hat{C} = \bigotimes_{x=1}^{V} \hat{U}$. Each block $\hat{U}$ is also block diagonal over the equivalence classes.

2. The projection operator, $\hat{\Gamma}$, periodically causes a partial collapse of the on-site superpositions. Therefore, a quantum computer with many qubits can simulate a quantum lattice gas with only short-term and short-range entanglement and coherence of qubits.

3. Streaming of complex amplitudes (or the associated qubits) occurs in analogy to streaming in a classical lattice gas and does not cause global entanglement in the quantum lattice gas because of the application of $\hat{\Gamma}$.

4. The quantum lattice gas can be understood as existing between two limits, a fully coherent quantum system and a classical system. And its single-particle distribution function, $f_a = |\omega_a|^2 = \langle q_a|\hat{n}|q_a \rangle = \langle \psi|\hat{n}_a|\psi \rangle$, has the form $f_a = 1/\left(\exp(\alpha\rho + \beta\hat{e}_a \cdot \vec{p} + \gamma E) + 1\right)$.

5. Like the lattice Boltzmann equation approach to simulate fluid dynamics, the quantum lattice gas is a noiseless method that directly codes the particle dynamics at the mesoscopic scale. However, unlike the lattice Boltzmann BGK collision operator, the quantum lattice-gas collision operator obeys detailed balance. Hence, the method is unconditionally stable.

6. The macroscopic hydrodynamic behavior is described by a viscous Navier-Stokes equation.

12 Closing Remarks

To mimic the behavior of other physical systems, quantum lattice gases need many qubits. A first generation quantum computer, with only two qubits, cannot test the behavior of the quantum lattice gas at the macroscopic scale. However, useful tests could be conducted on a network of these first generation machines to test the practicality of the quantum lattice-gas formalism. For example, we could test the reliability and computational speed of a network of quantum computers. It is reasonable to expect that the number of qubits will grow exponentially according to Moore's law as various quantum computer designs are realized over time.

We know from experience with classical lattice gases that although the underlying microscopic dynamics is reversible, dissipative shear viscosity arises at the macroscopic scale—entropy increases while at the same time information is conserved because of microscopic reversibility. The reason for this is that information, initially stored in the spatial correlations of arrangement of particle

occupancies, in time is transferred into high order particle-particle correlations. The same process should occur in a quantum lattice gas. We do not yet know, in a quantum lattice-gas setting, if there is a way to block this informational transfer mechanism and thereby reduce dissipation at the macroscopic scale.

Why consider constructing a quantum computer following the lattice gas paradigm, when a general purpose quantum computer could simulate a quantum lattice gas? The answer to this question is three-fold: (1) because any member of the appropriate unitary group associated with an equivalence class block of the collision operator is sufficient for the recover of Navier-Stokes hydrodynamics at the macroscopic scale, so the lattice-gas quantum computer is robust; (2) short-term coherence among only a small number of nearby qubits is needed; and (3) its behavior is predictable by analytic means.

The quantum lattice gas method can be straightforwardly applied to three-dimensional fluid simulations (the two-dimensional case was treated in this paper because of its simplicity) and also applied to model other physical systems. Lattice gases are a special case of cellular automata where conservations and detailed balance are imposed and an isotropic spatial lattice is used. With these few restrictions removed, the method presented in this paper represents a general computational system called a quantum cellular automaton.

13 Acknowledgements

References

[1] Wolfram, S.: Cellular automaton fluids 1: Basic theory. J. of Stat. Phys., **45**, No. 3/4 (1986) 471–526

[2] Frisch, U., Hasslacher, B., Pomeau, Y.: Lattice-gas automata for the navier-stokes equation. Phys. Rev. Lett., **56**, No. 14 (1986) 1505–1508

[3] Yepez, J.: Lattice-gas quantum computation. Inter. J. Theor. Phys, To appear, (1998) Proceeding of the 7th International Conference on the Discrete Simulation of Fluids, University of Oxford.

[4] Feynman, R. P.: Simulating physics with computers. Inter. J. Theor. Phys., **21**, No. 6/7 (1982) 467–488

[5] Benioff, P.: Quantum mechanical hamiltonian models of turing machines. J. of Stat. Phys., **29**, No. 3 (1982) 515–547

[6] Deutsch, D.: Quantum theory, the church-turing principle and the universal quantum computer. Proc. Roy. Soc., London, **A400** (1985) 97

[7] Margolus, M.: Quantum computation. In Daniel Greenberger, editor, *New Techniques and Ideas in Quantum Measurement Theory*, Annals of the New York Academy **480** (1985) 487–497

[8] Bennett, C. H.: Quantum information and computation. Physics Today, Oct (1995) 24–30

[9] Hey, A.J.G., Allen, R.W., editors: *Feynman Lectures on Computation*. The Advanced Book Program. Addison-Wesley Publishing Company, Inc. (1996)

[10] Cory,D.G., Fahmy, A.F., Havel, T.F.: Ensemble quantum computing by nuclear magnetic resonance spectroscopy. Harvard Univ. Center for Research in Comp. Tech., Aiken Comp. Lab., Tech Rep **TR-10-96** (1996)

[11] Calderbank, A.R., Shor.P.W.: Good quantum error correcting codes exist. *LANL archive: quant-ph/9512032* (1995)

[12] Seth Lloyd.: Quantum-mechanical computers. Physics Today, Oct (1995) 140–145

[13] Ekert, A., Jozsa, R.: Quantum computation and shor's factoring algorithm. Rev. of Mod. Phys., **68**, No. 3 (1996) 733–753

[14] Fredkin, E., Toffoli, T.: Conservative logic. Inter. J. Theor. Phys., **21**, No. 3/4 (1982) 219–253

[15] Bennett, C.H.: Logical reversibility of computation. IBM J. Res. Dev., **6** (1979) 525–532

[16] Bennett, C.H.: Thermodynamics of computation—a review. Inter. J. of Theor. Phys., **21** (1982) 219–253

[17] Sauro Succi.: Lattice boltzmann equation for quantum mechanics. Physica D, **69** (1993) 327–332

[18] Boghosian, B.M., Taylor, W.: A quantum lattice-gas model for the many-particle schrodinger equation in d-dimensions. Phys. Rev. E, **57**, No. 1 (1998) 54–66

[19] Yepez, J.: Lattice gas for superfluid helium ii. Inter. J. Theor. Phys. Accepted 1996. To Appear (1998). Presented at 6th Inter. Conf. on Discrete Models for Fluid Mech., Boston Univ. Center for Comp. Sci, Aug 1996.

[20] Hénon, M.: Viscosity of a lattice gas. In Gary D. Doolean, editor, *Lattice Gas Methods for Partial Differential Equations*, Santa Fe Institute, Addison-Wesley Publishing Company (1990) 179–207

[21] Frisch,U., d'Humières,D., Hasslacher,B., Lallemand, P., Pomeau,Y., Rivet, J.P.: Lattice gas hydrodynamics in two and three dimensions. Comp. Sys., **1** (1987) 649–707

[22] Yepez, J.: Lattice gas dynamics: Volume 1 viscous fluids. Technical Report **PL-TR-96-2122(I)**, Air Force Research Laboratory, AFRL/VSBE Hanscom AFB, MA, Nov (1996)

A   Single-Particle Distribution Function

The single-particle distribution function has the form

$$f(z_a) = \frac{1}{z_a + 1},\tag{93}$$

where the natural log of the *fugacity*

$$\ln z_a = \alpha\rho + \beta\hat{e}_a \cdot \vec{p} + \gamma E\tag{94}$$

is a linear combination of the conserved scalar quantities, the mass ρ, the momentum component $\hat{e}_a \cdot \vec{p}$ along the lattice direction $\hat{e}_a$, and the energy E at a lattice site. The real numbered coefficients α, β, and γ are free parameters that we will determine. It is convenient to define the momentum and energy independent part of the fugacity as

$$z_{\rm o} \equiv e^{\alpha\rho}.\tag{95}$$

Since $f_a(z_{\rm o}) = d$ is the reduced density, $d \equiv \frac{\rho}{mB}$, we must set

$$z_{\rm o} = \frac{1 - d}{d}.\tag{96}$$

This fixes the coefficient α. To fix the coefficients β and γ, we can specify two moments of the single-particle distribution function as constraint conditions. We begin by Taylor expanding the single-particle distribution function $f(z_a)$ about $z_{\rm o}$

$$f(z_a) = d + f'(z_{\rm o})\delta z + \frac{1}{2}f''(z_{\rm o})(\delta z^2) + \cdots.\tag{97}$$

The derivative of f evaluated at $z_{\rm o}$ are

$$f'(z) = \frac{-1}{(z+1)^2} \longrightarrow f'(z_{\rm o}) = -d^2\tag{98}$$

and

$$f''(z) = \frac{2}{(z+1)^3} \longrightarrow f''(z_{\rm o}) = 2d^3,\tag{99}$$

so

$$f(z_a) \cong d\left[1 - d\delta z + d^2(\delta z)^2\right].\tag{100}$$

To determine δz, we begin by writing the fugacity in series form

$$z_a = z_{\rm o}\left[\sum_{k=0}^{\infty}\frac{(\beta\hat{e}_a \cdot \vec{p})^k}{k!}\right]\left[\sum_{k=0}^{\infty}\frac{(\gamma E)^k}{k!}\right].\tag{101}$$

24

In the subsonic limit, $\vec{p} \ll mc$, keeping terms only to second order in the velocity, the fugacity becomes

$$z_a = z_\circ \left[1 + \beta \hat{e}_a \cdot \vec{p} + \frac{1}{2}(\beta \hat{e}_a \cdot \vec{p})^2 \right] (1 + \gamma E) + \mathcal{O}(v^3). \tag{102}$$

since $p \sim v$ and $E \sim v^2$. Then to second order in the velocity, the change in z_a is

$$\delta z_a \equiv z_a - z_\circ = \left(\frac{1-d}{d} \right) \left[\beta \hat{e}_a \cdot \vec{p} + \frac{1}{2}(\beta \hat{e}_a \cdot \vec{p})^2 + \gamma E \right] + \mathcal{O}(v^3) \tag{103}$$

and the square of the change is

$$(\delta z_a)^2 = \left(\frac{1-d}{d} \right)^2 \beta^2 \left(\hat{e}_a \cdot \vec{p} \right)^2 + \mathcal{O}(v^3). \tag{104}$$

Inserting the expressions for δz and $(\delta z)^2$ into the Taylor expansion of $f(z_a)$ we have

$$\begin{aligned} f(z_a) &= d \left\{ 1 - (1-d) \left[\beta \hat{e}_a \cdot \vec{p} + \frac{1}{2}(\beta \hat{e}_a \cdot \vec{p})^2 + \gamma E \right] + (1-d)^2 \left(\hat{e}_a \cdot \vec{p} \right)^2 \right\} \\ &= d \left[1 - (1-d) \left(\beta \hat{e}_a \cdot \vec{p} + \gamma E \right) + \frac{1}{2}(1-d)(1-2d)\beta^2 \left(\hat{e}_a \cdot \vec{p} \right)^2 \right] . \end{aligned} \tag{105}$$

We have the freedom to choose the coefficients β and γ to parameterized the distribution function as we see fit to satisfy any two constraints. Consider a parameterization that fixes the value of the coefficients β and γ by using the following moments for the mass density and momentum density

$$\rho = m \sum_{a=1}^{B} f_a \tag{106}$$

$$\rho \vec{v} = mc \sum_{a=1}^{B} \hat{e}_a f_a. \tag{107}$$

The parameterization may be termed the *non-Galilean parametrization*. Constraints (106) and (107) are typically used in the formulation of classical lattice gases. The single particle distribution function using this non-Galilean parameterization was first found in the mid 1980's by the US researchers Wolfram and Hasslacher and by the French researchers Frisch, d'Humières, Lallemand, Pomeau, and Rivet [1, 21]. Their derivation of (112) given below is different then the derivation presented in this section; they used only two free coefficients in the expression for the fugacity, one for the mass and the other for the momentum; whereas we use three free coefficients. The reason for using only two free parameters is that in the standard single-speed classical lattice-gas construction, the energy is degenerate with the mass, so it was deemed unnecessary to keep

a separate free coefficient for the energy. Using (106) and (107) as constraint equations gives us a non-unity density-dependent prefactor in the convective term in the hydrodynamic flow equation.

Inserting (105) into (107), the odd term in the distribution function expansion survives the first moment sum over lattice directions; the odd term is the one linear in the momentum. This fixes the value of β to be

$$\beta = -\frac{D}{1-d} \tag{108}$$

so the distribution function becomes

$$f_a = d\left[1 + D\hat{e}_a \cdot \vec{p} + \frac{D^2}{2}\frac{1-2d}{1-d}\left(\hat{e}_a \cdot \vec{p}\right)^2 + (1-d)\gamma E\right]. \tag{109}$$

Inserting (109) into (106), all the even terms that survive the sum over lattice directions must add to zero. This fixes the value of γ as follows

$$\frac{D}{2}\frac{1-2d}{1-d}p^2 - (1-d)\gamma E = 0 \tag{110}$$

or

$$\gamma E = D\frac{1-2d}{(1-d)^2}\frac{p^2}{2}. \tag{111}$$

Therefore, the non-Galilean parameterized distribution function is

$$f_a = d\left[1 + De_{ai}p_i + \frac{D(D+2)}{2}g(d)Q_{aij}p_ip_j\right], \tag{112}$$

where the density dependent prefactor $g(d)$ is defined

$$g(d) \equiv \frac{D}{D+2}\frac{1-2d}{1-d} \tag{113}$$

and the traceless second-rank tensor $\hat{Q}_a$ is defined

$$Q_{aij} \equiv e_{ai}e_{aj} - \frac{\delta_{ij}}{D}. \tag{114}$$

$\hat{Q}_a$ is an isotropic symmetric tensor. This mass-energy degeneracy leads to an anomalous description of the lattice-gas fluid's behavior. Let us see why. The second moment of (112) gives the momentum flux density

$$mc^2 \sum_{a=1}^{B} e_{ai}e_{aj}f_a = P\delta_{ij} + g\rho v_i v_j. \tag{115}$$

The density-dependent prefactor g appears in the nonlinear convective term, so this parametrization does indeed give rise to non-Galilean fluid flow. The pressure in (115) has a spurious quadratic velocity dependence

$$P = \rho c_s^2\left(1 - g\frac{v^2}{c^2}\right). \tag{116}$$

26

B   Determination of the Matrix Elements

For the triangular lattice, tensors made up of products of the lattice vectors are symmetric and isotropic [1]. We have the following identities

$$\langle 1 \mid \mathcal{L}_i \mid 1 \rangle = 0 \tag{117}$$

$$\langle 1 \mid \mathcal{L}_i\mathcal{L}_j \mid 1 \rangle = \frac{B}{D}\delta_{ij} \tag{118}$$

$$\langle 1 \mid \mathcal{L}_i\mathcal{L}_j\mathcal{L}_k \mid 1 \rangle = 0 \tag{119}$$

$$\langle 1 \mid \mathcal{L}_i\mathcal{L}_j\mathcal{L}_k\mathcal{L}_l \mid 1 \rangle = \frac{B}{D(D+2)}\left(\delta_{ij}\delta_{kl} + \delta_{ik}\delta_{jl} + \delta_{il}\delta_{jk}\right) \tag{120}$$

The Jacobion of the collision operator is circulant. Its eigenvectors corresponding to the nonzero eigenvalues span the *kinetic space*, which contains a *viscous subspace* characterized by a degenerate eigenvalue, denoted by κ_η [22]. The eigenvectors in the viscous subspace are $\mathcal{L}_i\mathcal{L}_j \mid 1 \rangle$, for $i \neq j$. Therefore, we have

$$\mathcal{J}\mathcal{L}_i\mathcal{L}_j \mid 1 \rangle = \kappa_\eta \mathcal{L}_i\mathcal{L}_j \mid 1 \rangle, \tag{121}$$

or inverting this over the kinetic viscous modes

$$\mathcal{J}^{-1}\mathcal{L}_i\mathcal{L}_j \mid 1 \rangle = \frac{1}{\kappa_\eta}\mathcal{L}_i\mathcal{L}_j \mid 1 \rangle. \tag{122}$$

Using these identities along with the epsilon expansion of $\mid \omega \rangle$, we can work out the value of the matrix elements which appear in the mass and momentum hydrodynamic equations of the quantum lattice gas at the macroscopic scale. We have

$$\begin{aligned}
\langle \omega^{(0)} \mid \mathcal{L}_i\mathcal{L}_j \mid \omega^{(0)} \rangle &= d\langle 1 \mid \mathcal{L}_i\mathcal{L}_j \mid 1 \rangle + \frac{dD}{c}\langle 1 \mid \mathcal{L}_i\mathcal{L}_j\mathcal{L}_k \mid 1 \rangle v_k + \\
&\quad \frac{gdD(D+2)}{2c^2}\langle 1 \mid \mathcal{L}_i\mathcal{L}_j\left(\mathcal{L}_k\mathcal{L}_l - \frac{\delta_{kl}}{D}\right) \mid 1 \rangle v_k v_l \\
&= \frac{dB}{D}\delta_{ij} + \frac{gdB}{2c^2}\left(\delta_{ij}\delta_{kl} + \delta_{ik}\delta_{jl} + \delta_{il}\delta_{jk}\right)v_k v_l - \frac{gd(D+2)B}{2Dc^2}\delta_{ij}v^2 \\
&= \frac{dB}{D}\left(1 - g\frac{v^2}{c^2}\right)\delta_{ij} + gdB\frac{v_i v_j}{c^2}. \tag{123}
\end{aligned}$$

$$\begin{aligned}
\langle \omega^{(0)} \mid \mathcal{L}_i\mathcal{L}_j \mid \partial_i\partial_j\omega^{(0)} \rangle &= \frac{dD}{2c}\langle 1 \mid \mathcal{L}_i\mathcal{L}_j\mathcal{L}_k \mid 1 \rangle \partial_i\partial_j v_k \\
&= 0. \tag{124}
\end{aligned}$$

$$\begin{aligned}
\langle \omega^{(0)} \mid \mathcal{L}_i\mathcal{L}_j\mathcal{L}_k \mid \partial_j\partial_k\omega^{(0)} \rangle &= \frac{dD}{2c}\langle 1 \mid \mathcal{L}_i\mathcal{L}_j\mathcal{L}_k\mathcal{L}_l \mid 1 \rangle \partial_j\partial_k v_l \\
&= \frac{dB}{2c(D+2)}\left(\delta_{ij}\delta_{kl} + \delta_{ik}\delta_{jl} + \delta_{il}\delta_{jk}\right)\partial_j\partial_k v_l \\
&= \frac{dB}{2c(D+2)}\left(2\partial_i\partial_k v_k + \partial^2 v_i\right). \tag{125}
\end{aligned}$$

27

$$\langle \omega^{(0)} \mid \mathcal{L}_i \mathcal{J}^{-1} \mathcal{L}_j \mid \partial_j \omega^{(0)} \rangle = \frac{dD}{2c} \langle 1 \mid \mathcal{L}_i \mathcal{J}^{-1} \mathcal{L}_j \mathcal{L}_k \mid 1 \rangle \partial_j v_k$$

$$= \frac{dD}{2c\kappa_\eta} \langle 1 \mid \mathcal{L}_i \mathcal{L}_j \mathcal{L}_k \mid 1 \rangle \partial_j v_k$$

$$= 0. \tag{126}$$

$$\langle \omega^{(0)} \mid \mathcal{L}_i \mathcal{L}_j \mathcal{J}^{-1} \mathcal{L}_k \mid \partial_k \omega^{(0)} \rangle = \frac{dD}{2c} \langle 1 \mid \mathcal{L}_i \mathcal{L}_j \mathcal{J}^{-1} \mathcal{L}_k \mathcal{L}_l \mid 1 \rangle \partial_k v_l$$

$$= \frac{dD}{2c\kappa_\eta} \langle 1 \mid \mathcal{L}_i \mathcal{L}_j \mathcal{L}_k \mathcal{L}_l \mid 1 \rangle \partial_k v_l$$

$$= \frac{dB}{2c\kappa_\eta(D+2)} \left(\delta_{ij}\delta_{kl} + \delta_{ik}\delta_{jl} + \delta_{il}\delta_{jk} \right) \partial_k v_l$$

$$= \frac{dB}{2c\kappa_\eta(D+2)} \left(\partial_k v_k \delta_{ij} + \partial_i v_j + \partial_j v_i \right). \tag{127}$$

REPORT DOCUMENTATION PAGE

1. REPORT DATE (DD-MM-YYYY)	2. REPORT TYPE	3. DATES COVERED (From - To)
17-8-2005	REPRINT	

4. TITLE AND SUBTITLE	5a. CONTRACT NUMBER
Quantum Computation of Fluid Dynamics	
	5b. GRANT NUMBER
	5c. PROGRAM ELEMENT NUMBER 61102F

6. AUTHOR(S)	5d. PROJECT NUMBER
Jeffrey Yepez	2304
	5e. TASK NUMBER OT
	5f. WORK UNIT NUMBER B1

7. PERFORMING ORGANIZATION NAME(S) AND ADDRESS(ES)	8. PERFORMING ORGANIZATION REPORT NUMBER
Air Force Research Laboratory/VSBYA 29 Randolph Road Hanscom AFB MA 01731-3010	AFRL-VS-HA-TR-2005-1092

9. SPONSORING / MONITORING AGENCY NAME(S) AND ADDRESS(ES)	10. SPONSOR/MONITOR'S ACRONYM(S)
	11. SPONSOR/MONITOR'S REPORT NUMBER(S)

12. DISTRIBUTION / AVAILABILITY STATEMENT

Approved for Public Release; Distribution Unlimited.

13. SUPPLEMENTARY NOTES

14. ABSTRACT

Presented is a quantum lattice gas for Navier-Stokes fluid dynamics simulation. The quantum lattice-gas transport equation at the microscopic scale is presented as a generalization of the classical lattice-gas transport equation. A special type of quantum computer network is proposed that is suitable for implementing the quantum lattice gas. The quantum computer network undergoes a partial collapse of the wavefunction at every time step of the dynamical evolution. Each quantum computer in the network comprises only a few qubits, which are entangled for only a short time period. A Chapman-Enskog type analysis of the quantum computer network indicates that the total system of qubits behaves exactly like a viscous lattice-gas fluid at the macroscopic scale. Because of the quantum mechanical nature of the scattering process, superposition of outgoing collisional possibilities occurs. The quantum lattice gas obeys detail balance in its collisions and is therefore an unconditionally stable algorithm for fluid dynamics simulation.

15. SUBJECT TERMS

Quantum lattice gas   Navier-Stokes fluid
Microscopic scale

16. SECURITY CLASSIFICATION OF:			17. LIMITATION OF ABSTRACT	18. NUMBER OF PAGES	19a. NAME OF RESPONSIBLE PERSON
a. REPORT UNCLAS	**b. ABSTRACT** UNCLAS	**c. THIS PAGE** UNCLAS	SAR		Jeffrey Yepez
					19b. TELEPHONE NUMBER (include area code) 781-377-5957